Experimental Results of Spherical Arrays of Circular Waveguide and Microstrip Antennas

Vanja Mandrić, Slavko Rupčić, Danijel Pilski
University J.J.Strossmayer of Osijek, Faculty of Electrical Engineering, Osijek, Croatia
vanja.mandric@etfos.hr, slavko.rupcic@etfos.hr, danijel.pilski@etfos.hr

Abstract – Arrays of circular waveguide and microstrip antennas on spherical surface are measured. The radiation pattern of a two experimental models of antenna arrays on spherical surface is obtained experimentally and is compared with theoretical patterns in order to verify theoretical results, without intention to improving the best radiation characteristics of a developed laboratory models. Arrays are analyzed using the spectral-domain approach and moment method. Measurements were not performed in a well-defined anechoic environment.

Keywords - radiation pattern, spherical array, waveguide antenna, microstrip antenna, microstrip array

I. Introduction

An array of antennas disposed on the surface of a sphere is of importance because such an array provides wide hemispherical scan coverage with low grating lobe levels. Spherical array antennas combine the capabilities of array antennas with the optimal geometry to achieve omni-directional coverage.

The array was modeled using a previously presented computer programs based on the method of moments in spectral domain [1], [2].

In the process of verifying theoretical results we built two experimental models and validated theoretical results by comparing the results to the measurements performed on the developed laboratory models.

We also discuss the results of an experimental investigation of a two spherical arrays. First array consisting of circular waveguide elements with apertures on a hemispherical ground surface and second consisting of circular microstrip antennas on hemispherical ground surface.

II. Far Field Calculation

Since the radiating structure is spherical, the problem is defined in the spherical coordinate system and this spectrum is obtained by applying the vector-Legendre transformation to the equivalent current at waveguide aperture. An electrical field radiated by the current shell on the spherical surface in homogeneous media is:

$$\mathbf{E}(r,\theta,\phi)=\sum_{m=-\infty}^{\infty}\sum_{n=|m|}^{\infty}\overline{\overline{\mathbf{L}}}(n,m,\theta)\tilde{\overline{\overline{\mathbf{G}}}}(n,m,r\,|\,r_s)\tilde{\mathbf{C}}(r,n,m)e^{jm\phi}, \qquad (1)$$

where $\tilde{\overline{\overline{\mathbf{G}}}}(n,m,r\,|\,r_s)$ is a spectral domain dyadic Green's function for a grounded spherical surface, $\overline{\overline{\mathbf{L}}}(n,m,\theta)$ is the kernel of the vector - Legendre transformation and $\tilde{\mathbf{C}}(r,n,m)$ is a spectral domain current placed at each antenna element.

The kernel of the integral operator is Green's function, which is different for different structures.

The appropriate spectral-domain Green's function of a multilayer spherical structure is calculated using the G1DMULT algorithm [1], [3].

The radiation pattern of the array is obtained as a superposition of fields excited by each waveguide aperture (placed on spherical surface at the point with coordinate (α_n , β_n)) :

$$E_{\theta,\alpha_n,\beta_n}(\theta,\phi)=-\frac{\sin\alpha_n\sin(\phi-\beta_n)}{\sin\theta'}E_{\phi}(\theta',\phi)$$
$$-\frac{\cos\theta\sin\alpha_n\cos(\phi-\beta_n)-\sin\theta\cos\alpha_n}{\sin\theta'}E_{\theta}(\theta',\phi') \qquad (2)$$

$$E_{\phi,\alpha_n,\beta_n}(\theta,\phi)=\frac{\sin\alpha_n\sin(\phi-\beta_n)}{\sin\theta'}E_{\theta}(\theta',\phi')$$
$$-\frac{\cos\theta\sin\alpha_n\cos(\phi-\beta_n)-\sin\theta\cos\alpha_n}{\sin\theta'}E_{\phi}(\theta',\phi') \qquad (3)$$

where α_n and β_n are the θ and ϕ coordinates of each antenna element in the global coordinate system [4],[5].

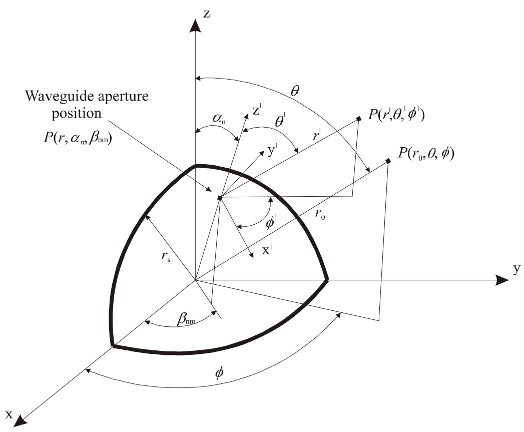

Figure 1. Global and local coordinate system [2].

We introduced local coordinate systems with the origin located at the center of each antenna element (shown in Fig.1).

The complete pattern expression of the field produced by the array given as:

$$\mathbf{E}(\theta,\phi) = \sum_{n,m} \mathbf{E}_{\alpha_n \beta_{nm}}(\theta,\phi) \qquad (4)$$

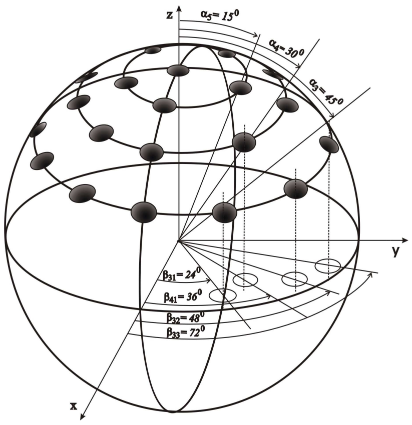

Figure 2. Geometrical representation of the antenna element distribution on spherical surface [2].

III. Experimental Models Of A Spherical Array

A fabricated hemispherical array antenna MODEL I is shown in Fig.3, and its design specification are listed in Tab.1.

The considered antennas are designed with circular waveguides used as antenna elements placed on the spherical structure. The second array (MODEL II) is shown in Fig.4., and its design specifications are listed in Tab.2.

The antenna elements are placed at equidistant position on the (grounded) surface of the icosahedron (Fig.2.).

Circular waveguides and patches used as antenna elements are fed by the coaxial lines at one point to generate linear polarization.

TABLE I. Design specifications of hemispherical array – model I (Fig.3.)

Parameter	**Values / Description**
Antenna Element	Circular Waveguide
Diameter of Element	120 ± 2 mm
Arangement of Elements	Icosahedral (P_n= 4)
Number of Elements	6
Element Positions	*Polar:* $\alpha_6=0^0$, $\beta_{61}=0^0$ *First ring:* $\alpha_5=56^0$, $\beta_{51}=36^0$, $\beta_{52}=108^0$, $\beta_{53}=180^0$, $\beta_{54}=252^0$, $\beta_{55}=324^0$
Element Spacing	Minimum 1.7 λ_0
Diameter of Sphere	600 ± 5 mm
Frequency Range for Single Mod – TE_{11}	1.47 – 1.91 GHz

TABLE II. Design specifications of hemispherical array – model II (Fig.4.)

Parameter	**Values / Description**
Antenna Element	Circular Microstrip
Diameter of Element	53 ±0.5 mm
Arangement of Elements	Icosahedral (P_n= 4)
Number of Elements	31
Element Positions	*Polar:* $\alpha_6=0^0$, $\beta_{61}=0^0$ *First ring:* $\alpha_5=15^0$, $\beta_{51}=0^0$, $\beta_{52}=72^0$, $\beta_{53}=144^0$, $\beta_{54}=216^0$, $\beta_{55}=288^0$ *Second ring:* $\alpha_4=30^0$, $\beta_{41}=0^0$, $\beta_{42}=36^0$, $\beta_{43}=72^0$, $\beta_{44}=108^0$, $\beta_{45}=144^0$, $\beta_{46}=180^0$, $\beta_{47}=216^0$, $\beta_{48}=252^0$, $\beta_{49}=288^0$, $\beta_{410}=324^0$, *Third ring:* $\alpha_3=45^0$, $\beta_{31}=0^0$, $\beta_{32}=24^0$, $\beta_{33}=48^0$, $\beta_{34}=72^0$, $\beta_{35}=96^0$, $\beta_{36}=120^0$, $\beta_{37}=144^0$, $\beta_{38}=168^0$, $\beta_{39}=192^0$, $\beta_{310}=216^0$, $\beta_{311}=240^0$, $\beta_{312}=264^0$, $\beta_{313}=288^0$, $\beta_{314}=312^0$, $\beta_{315}=336^0$
Element Spacing	Minimum 0.5 λ_0
Thickness of the Substrate	1.06 ± 0.02 mm
Relative Dielectric Constant of the Substrate	4.48
Diameter of Sphere	600 ± 5 mm

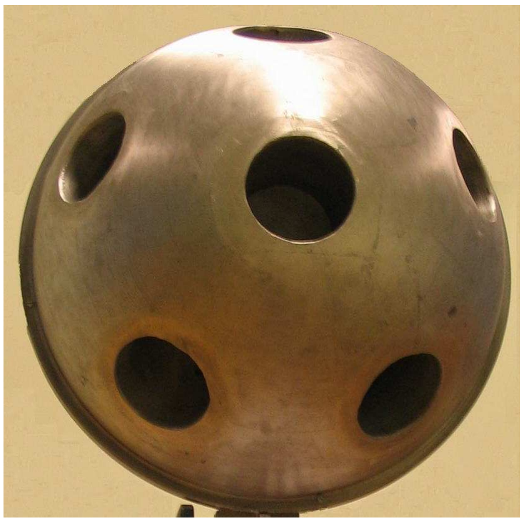

Figure 3. Spherical experimental model (MODEL I) with 6 antenna elements – circular waveguides [2] , [6].

Further, normalized free - space radiation patterns were calculated and measured at the frequencies: f = 1.75 GHz – MODEL I; f = 1.54 GHz – MODEL II.

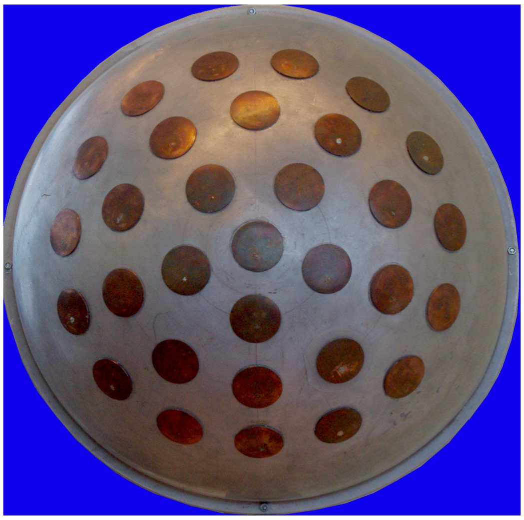

Figure 4. Spherical experimental model (MODEL II) with 31 antenna elements - circular microstrip antennas.

The first antenna subarray (MODEL II) consisting of three circular microstrip antennas on the positions: $\alpha_6=0^0$, $\beta_{61}=0^0$, $\alpha_5=15^0$, $\beta_{51}=0^0$, $\beta_{52}=72^0$.

The second antenna subarrays (MODEL II) consisting of three circular microstrip antenna on the positions: $\alpha_6=0^0$, $\beta_{61}=0^0$, $\alpha_5=15^0$, $\beta_{51}=0^0$, $\alpha_4=30^0$, $\beta_{41}=0^0$. We forms a beam by exciting a 3 – element subarray and changes direction of maximum radiation by phase compensation. The input power was distributed to each element of the subarrays first, with equal phase and amplitude, and second, with phase delay compensation and constant (uniform) amplitude.

IV. Theoretical And Measured Results

In these experiments we excited a particular section of the spherical surface centered around the maximum direction of the beam (θ_{max} and ϕ_{max}), and move the activated portion on the surface for beam steering purposes.

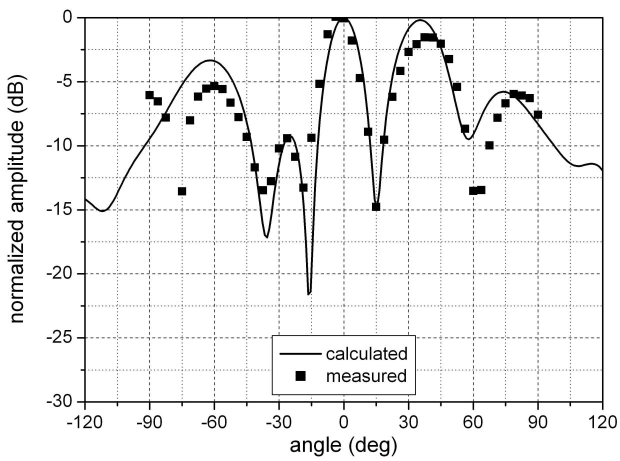

a)

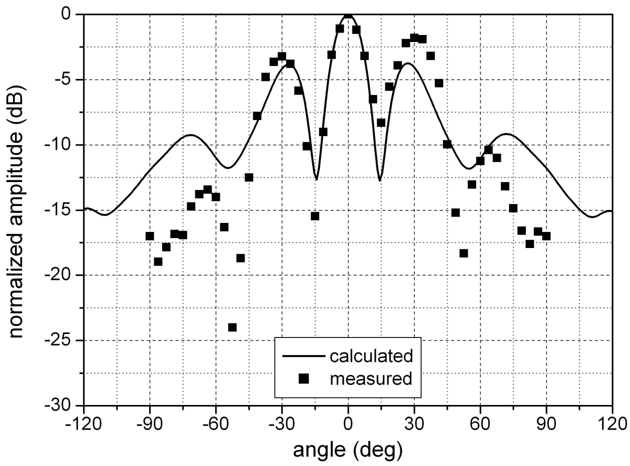

b)

Figure 5. Normalized radiation pattern of six circular waveguide array on a spherical surface – MODEL I: a) E - plane; b) H – plane; (α_6=0 0, β_{61}=0 0, $\alpha_5=15^0$, $\beta_{51}=36^0$, $\beta_{52}=108^0$, $\beta_{53}=180^0$, $\beta_{54}=252^0$, $\beta_{55}=324^0$); max radiation angle: $\theta_{max}=0^0$, $\varphi_{max}=0^0$; non-phased.

The considered an antenna arrays transmitting a wave into the far field region where strength of its field is to be measured. Excitation of antenna elements (waveguides and microstrip antennas) is constant and uniform and elements are progressively phased.

The antenna arrays were oriented in a fixed position and both E- and H- plane patterns have been recorded. All array configurations are excited with and without phase shift.

Further, the radiation pattern of microstrip antennas were measured with two different direction of maximal radiation (first direction: $\theta_{max}=0^0$, $\phi_{max}=0^0$, and second direction: direction of the excited subarray center).

Normalized radiation pattern were measured with and without the necessary phasing for the orientation of the beam.

The radiation patterns produced by two experimental models were measured over the azimuthal angle range -90^0 to 90^0.

Theoretical and measured free-space normalized radiation patterns in two orthogonal planes of circular waveguide antenna array (MODEL I) on the spherical surface are shown in Fig. 5 and 6. The direction of maximum radiation is the north pole direction. In order to obtain in-phase addition of antenna elements, a feed network with appropriate phasing is provided. The side lobes appears around $\pm$ 30^0, they are significant high (Fig.5), but the side lobe amplitude dropped by phase delay (Fig.6). We can see that matching of theoretical and experimental results is very good across the region of main beam (angles < 30^0) but in area close to the edges of the experimental model (angles > 60^0) theoretical and experimental results are not in a good agreement.

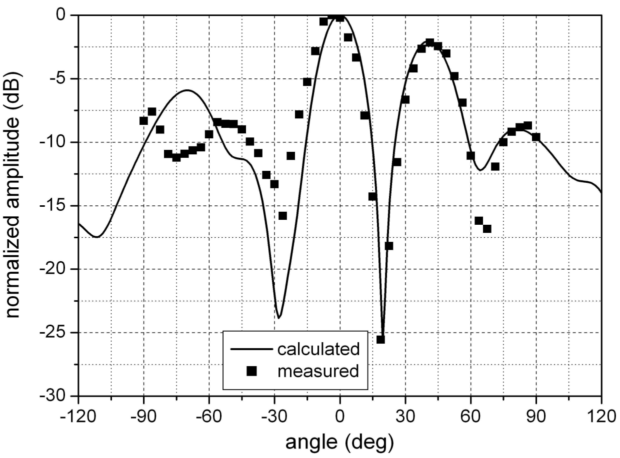

a)

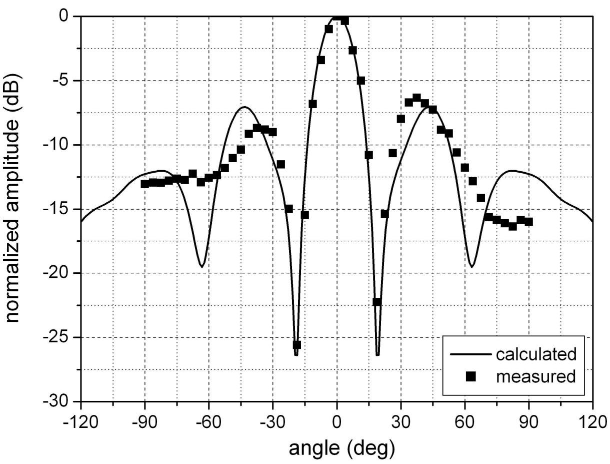

b)

Figure 6. Normalized radiation pattern of six circular waveguide array on a spherical surface – MODEL I: a) E - plane; b) H – plane; (α_6=0^0, β_{61}=0^0, α_5=15^0,β_{51}=36^0, β_{52}=108^0, β_{53}=180^0, $\beta_{54}{}^0$, β_{55}=324^0); max radiation angle: θ_{max}=0^0, φ_{max}=0^0; phased.

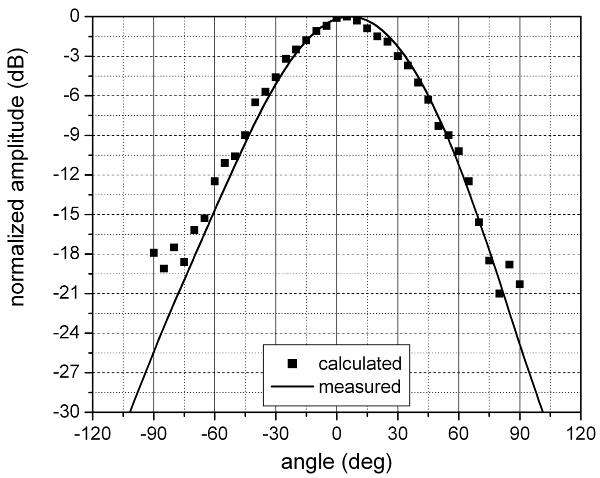

a)

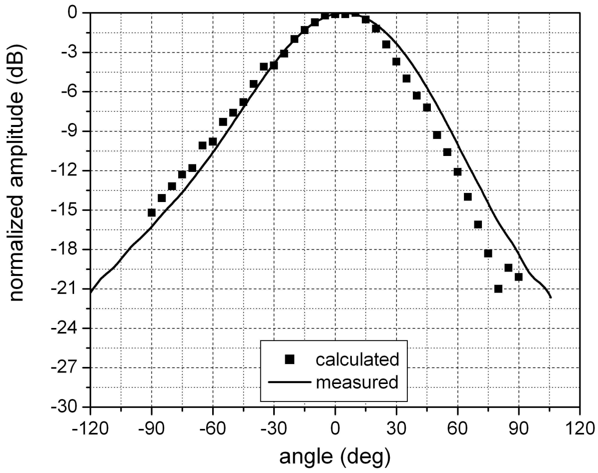

b)

Figure 7. Normalized radiation pattern of three circular microstrip subarray on a spherical surface – MODEL II: a) E - plane; b) H – plane; (α_6=0^0, β_{61}=0^0, α_5=15^0, β_{51}=0^0, β_{52}=72^0); max radiation angle: θ_{max}=0^0, φ_{max}=0^0; non-phased.

Figures 7, 9 and 11 show free-space normalized radiation patterns of the first antenna subarrays (Fig.8) consisting of three circular microstrip antenna with two different maximum radiation angle.

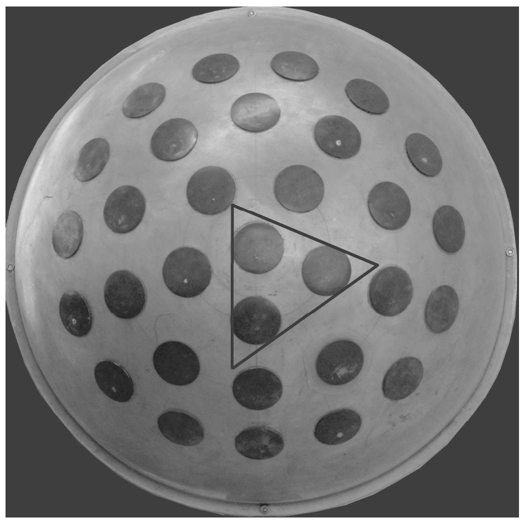

Figure 8. First subarray of the spherical experimental model. (MODEL II)

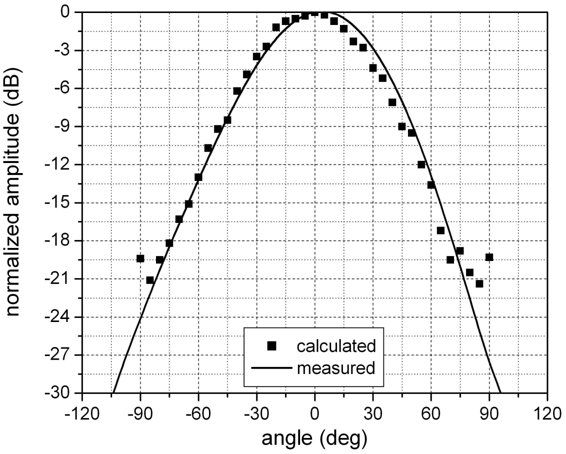

a)

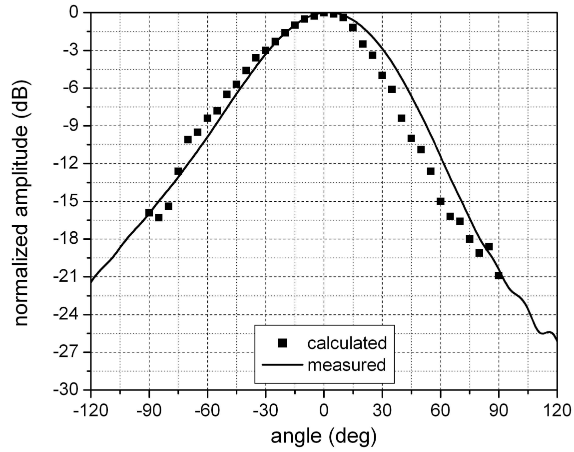

b)

Figure 9. Normalized radiation pattern of three circular microstrip subarray on a spherical surface – MODEL II: a) E - plane; b) H – plane; (α_6=0^0, β_{61}=0^0, α_5=15^0, β_{51}=0^0, β_{52}=72^0); max radiation angle: θ_{max}=0^0, φ_{max}=0^0; phased.

Figures 12, 13, 14 and 15 show normalized radiation patterns of the second antenna subarrays (Fig.10) in two orthogonal planes. As we can see the sidelobe levels decrease for all phased subarrays.

Also, radiation patterns are not optimal because we have not achieved an optimal solution regarding the inter-element distances and number of excited antenna elements. We have compared measured and theoretical results in order to verify theoretical results, without intention to improving the best radiation characteristics of developed experimental models. Moreover, we achieve a very good agreement between the theoretical and the measured normalized radiation pattern regarding the main beam and side lobes.

Figure 10. Second subarray of the spherical experimental model. (MODEL II)

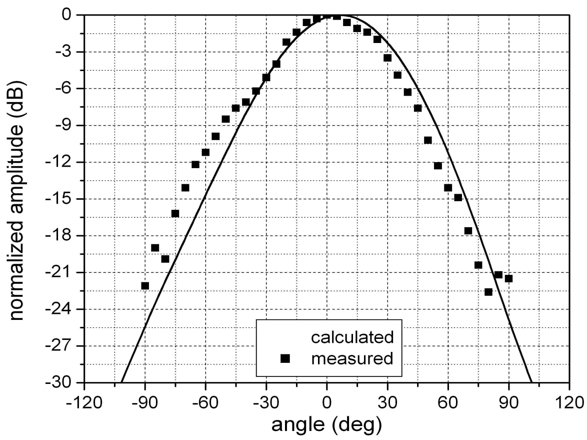

a)

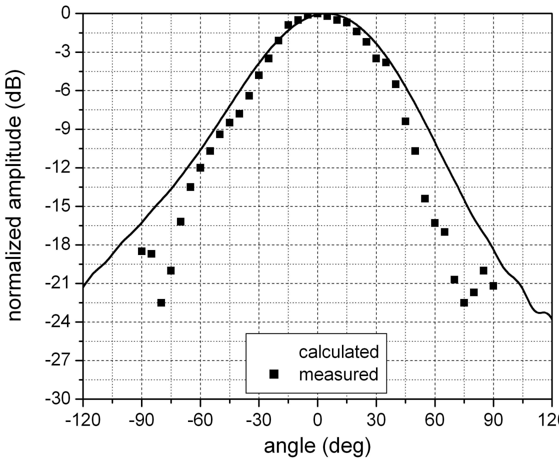

b)

Figure 11. Normalized radiation pattern of three circular microstrip subarray on a spherical surface – MODEL II: a) E - plane; b) H – plane; (α_6=0^0, β_{61}=0^0, α_5=15^0, β_{51}=0^0, β_{52}=72^0); max radiation angle: θ_{max}=7.5^0, φ_{max}=36^0; non-phased.

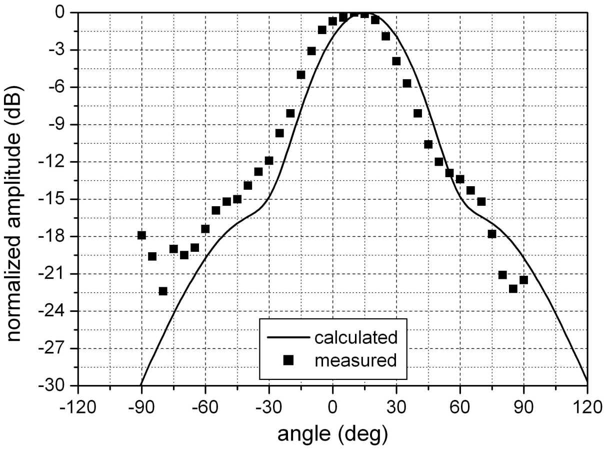

a)

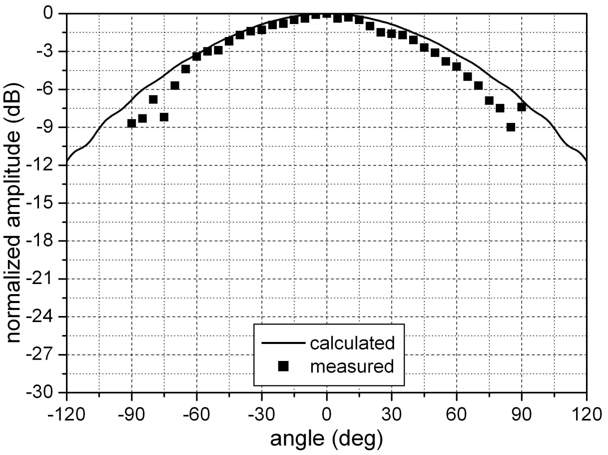

b)

Figure 12. Normalized radiation pattern of three circular microstrip subarray on a spherical surface – MODEL II: a) E - plane; b) H – plane; (α_6=0^0, β_{61}=0^0, α_5=15^0, β_{51}=0^0, α_4=30^0, β_{41}=0^0); max radiation angle: θ_{max}=0^0, φ_{max}=0^0; non-phased.

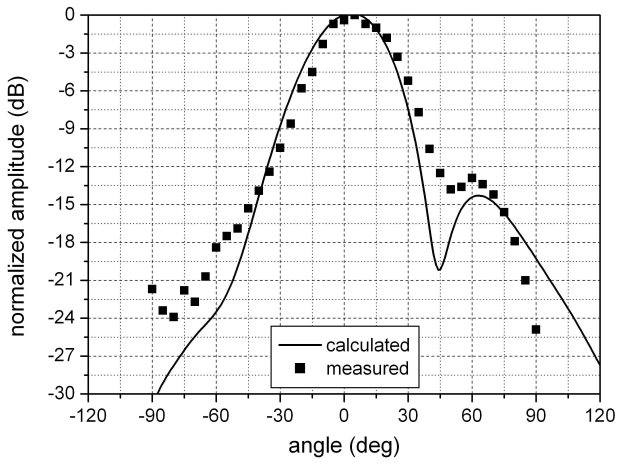

a)

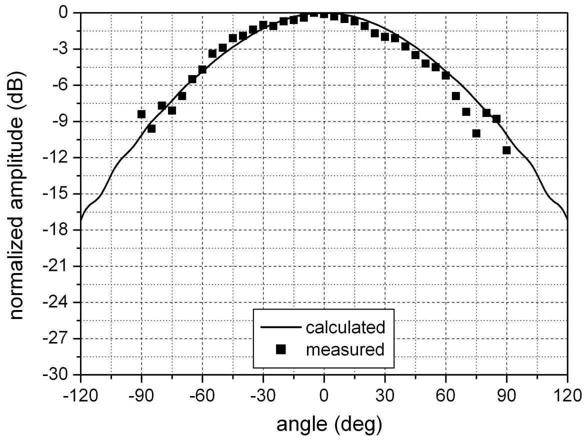

b)

Figure 13. Normalized radiation pattern of three circular microstrip subarray on a spherical surface – MODEL II: a) E - plane; b) H – plane; (α_6=0^0, β_{61}=0^0, α_5=15^0, β_{51}=0^0, α_4=30^0, β_{41}=0^0); max radiation angle: θ_{max}=0^0, φ_{max}=0^0; phased.

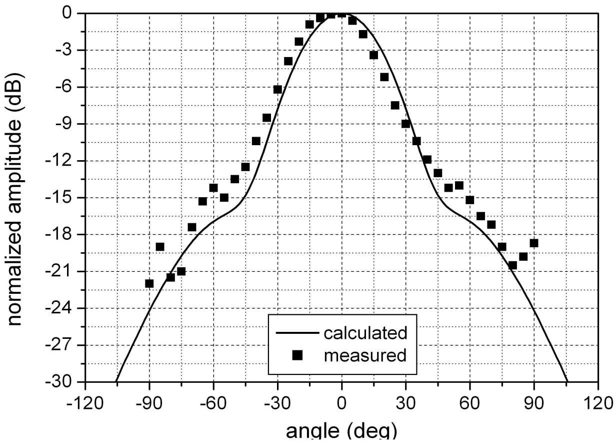

a)

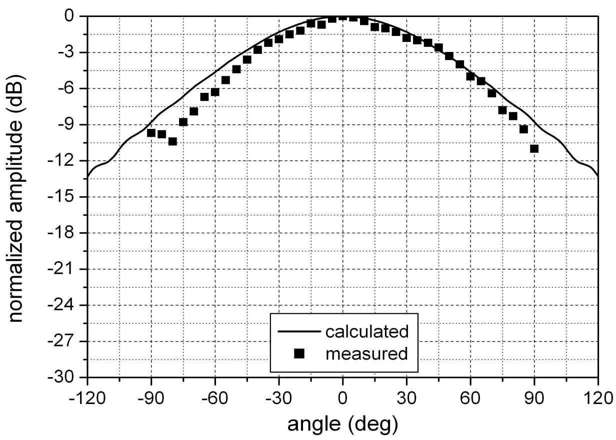

b)

Figure 14. Normalized radiation pattern of three circular microstrip subarray on a spherical surface – MODEL II: a) E - plane; b) H – plane; (α_6=0^0, β_{61}=0^0,α_5=15^0, β_{51}=0^0, α_4=30^0, β_{41}=0^0); max radiation angle: θ_{max}=15^0, φ_{max}=0^0;   non-phased.

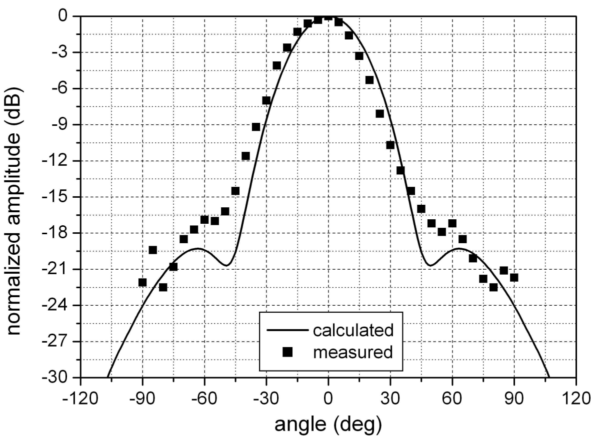

a)

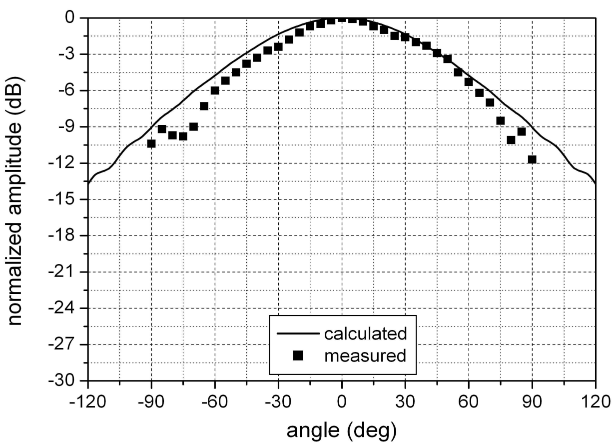

b)

Figure 15. Normalized radiation pattern of three circular microstrip subarray on a spherical surface – MODEL II: a) E - plane; b) H – plane; (α_6=0^0, β_{61}=0^0, α_5=15^0, β_{51}=0^0, α_4=30^0, β_{41}=0^0); max radiation angle: θ_{max}=15^0, φ_{max}=0^0; phased.

V. CONCLUSION

In this paper, we have shown the normalized free-space radiation pattern of two spherical antenna arrays.

Analysis of the arrays was made with the developed moment method programs.

A computer programs were developed to calculate the far-field radiation patterns of the phase/non-phase compensated spherical arrays with two types of antenna elements: circular waveguides and microstrip patches. The results obtained from the theoretical investigation are verified by comparison with measured results.

The errors in the measured results appear due to experimental model errors, diffraction from the edges of the semi-spherical surface and reflections inside the measurement room which is not a well-defined anechoic chamber.

REFERENCES

[1] Z. Sipus, P.-S. Kildal, R. Leijon and M. Johansson, "An algorithm for calculating Green's functions for planar, circular cylindrical and spherical multilayer substrates," *Applied Computational Electromagnetics Society Journal*, Vol. 13, pp. 243-254,1998.

[2] S. Rupcic, "Circular Waveguide Antenna Arrays on Spherical Structures", PhD Thesis, *University of Zagreb, Faculty of Electrical Engineering and Computing*, Zagreb, 2009.

[3] P.-S. Kildal and J. Sanford, "Analysis of conformal antennas by using spectral domain techniques for curved structures", *Proccedings of COST 245 - ESA workshop on active antennas*, Noordwijk, pp. 17-26, 1996.

[4] D. L. Sengupta, T. M. Smith, and R. W. Larson, "Radiation Characteristics of Spherical Array of Circularly Polarized Elements", *IEEE Trans. on Antennas and Propagation*, Vol. 16, pp. 2-7, Jan. 1968.

[5] Z. Sipus, S. Rupcic, M. Lanne and L. Josefsson, "Analysis of Circular and Spherical Array of Waveguide Elements Covered With Radome", *Proceedings of IEEE International Symposium on Antennas and Propagation*, *Boston*, USA, pp. II 350-353, 2001.

[6] S. Rupcic, V. Mandric and D. Vinko, "Radiation Pattern of Waveguide Antenna Arrays on Spherical Surface – Experimental Results", *International Journal of Electricaland Computer Engineering Systems*,, Vol. 1, No. 1, pp. 31-36, 2010.